

# Classical double-well systems coupled to finite baths

Hideo Hasegawa\*

*Department of Physics, Tokyo Gakugei University, Koganei, Tokyo 184-8501, Japan*

(Dated: May 15, 2022)

## Abstract

We have studied properties of a classical  $N_S$ -body double-well system coupled to an  $N_B$ -body bath, performing simulations of  $2(N_S + N_B)$  first-order differential equations with  $N_S \simeq 1 - 10$  and  $N_B \simeq 1 - 1000$ . A motion of Brownian particles in the absence of external forces becomes chaotic for appropriate model parameters such as  $N_B$ ,  $c_o$  (coupling strength), and  $\{\omega_n\}$  (oscillator frequency of bath): For example, it is chaotic for a small  $N_B$  ( $\lesssim 100$ ) but regular for a large  $N_B$  ( $\gtrsim 500$ ). Detailed calculations of the stationary energy distribution of the system  $f_S(u)$  ( $u$ : an energy per particle in the system) have shown that its properties are mainly determined by  $N_S$ ,  $c_o$  and  $T$  (temperature) but weakly depend on  $N_B$  and  $\{\omega_n\}$ . The calculated  $f_S(u)$  is analyzed with the use of the  $\Gamma$  distribution. Difference and similarity between properties of double-well and harmonic-oscillator systems coupled to finite bath are discussed.

PACS numbers: 05.40.-a, 05.70.-a, 05.10.Gg

---

\*hideohasegawa@goo.jp

## I. INTRODUCTION

Many studies have been made with the use of a model describing a classical or quantum open system which is coupled to baths consisting of a collection of harmonic oscillators. Such a model is conventionally referred to as the Caldeira-Leggett (CL) model [1, 2], although equivalent models had been proposed earlier by Magalinskii [3] and Ullersma [4]. From the CL model, we may derive the Langevin model with dissipation and diffusion (noise) terms. Originally the CL model was introduced for  $N_B$ -body bath with  $N_B \rightarrow \infty$ , for which the Ohmic and Drude-type spectral densities with continuous distributions are adopted. Furthermore in the original CL model, the number of particles in a systems,  $N_S$ , is taken to be unity ( $N_S = 1$ ). We expect that a generic open system may contain any number of particles and that a system may be coupled to a bath consisting of finite harmonic oscillators in general. In recent years, the CL model has been employed for a study of properties of open systems with finite  $N_S$  and/or  $N_B$  [5–13]. Specific heat anomalies of quantum oscillator (system) coupled to finite bath have been studied [5, 6, 12]. A thermalization [7, 8], energy exchange [9], dissipation [11] and the Jarzynski equality [13, 14] in classical systems coupled to finite bath have been investigated.

In a previous paper [10], we have studied the  $(N_S + N_B)$  model for finite  $N_S$ -body systems coupled to baths consisting of  $N_B$  harmonic oscillators. Our study for open harmonic oscillator systems with  $N_S \simeq 1 - 10$  and  $N_B \simeq 10 - 1000$  has shown that stationary energy distribution of the system has a significant and peculiar dependence on  $N_S$ , but it weakly depends on  $N_B$  [10]. These studies mentioned above [5–13] have been made for harmonic-oscillator systems with finite  $N_S$  and/or  $N_B$ .

Double-well potential models have been employed in a wide range of fields including physics, chemistry and biology (for a recent review on double-well system, see Ref. [15]). Various phenomena such as the stochastic resonance (SR), tunneling through potential barrier and thermodynamical properties [16] have been studied. The CL model for the double-well systems with  $N_S = 1$  and  $N_B = \infty$  has been extensively employed for a study on the SR [17]. Properties of SR for variations of magnitude of white noise [17–20] and relaxation time of colored noise [21, 22] have been studied. However, studies for open double-well systems with finite  $N_S$  and/or  $N_B$  have not been reported as far as we are aware of. It would be interesting and worthwhile to study open classical double-well systems described by the

$(N_S + N_B)$  model with finite  $N_S$  and  $N_B$ , which is the purpose of the present paper.

The paper is organized as follows. In Sec. II, we briefly explain the  $(N_S + N_B)$  model proposed in our previous study [10]. In Sec. III, direct simulations (DSs) of  $2(N_S + N_B)$  first-order differential equations for the adopted model have been performed. Dynamics of a single double-well system ( $N_S = 1$ ) coupled to a finite bath ( $2 \leq N_B \leq 1000$ ) in the phase space is investigated (Sec. III B). We study stationary energy distributions in the system and bath, performing detailed DS calculations, changing  $N_S$ ,  $N_B$ , the coupling strength and the distribution of bath oscillators (Sec. III C). Stationary energy and position distributions obtained by DSs are analyzed in Sec. IV. The final Sec. V is devoted to our conclusion.

## II. ADOPTED $(N_S + N_B)$ MODEL

We consider a system including  $N_S$  Brownian particles coupled to a bath consisting of independent  $N_B$  harmonic oscillators. We assume that the total Hamiltonian is given by [10]

$$H = H_S + H_B + H_I, \quad (1)$$

with

$$H_S = \sum_{k=1}^{N_S} \left[ \frac{P_k^2}{2M} + V(Q_k) \right], \quad (2)$$

$$H_B = \sum_{n=1}^{N_B} \left[ \frac{p_n^2}{2m} + \frac{m\omega_n^2}{2} q_n^2 \right], \quad (3)$$

$$H_I = \frac{1}{2} \sum_{k=1}^{N_S} \sum_{n=1}^{N_B} c_{kn} (Q_k - q_n)^2, \quad (4)$$

where  $H_S$ ,  $H_B$  and  $H_I$  express Hamiltonians for the system, bath and interaction, respectively. Here  $M$  ( $m$ ) denotes the mass,  $P_k$  ( $p_n$ ) the momentum,  $Q_k$  ( $q_n$ ) position of the oscillator in the system (bath),  $V(Q_k)$  signifies the potential in the system,  $\omega_n$  stands for oscillator frequency in the bath, and  $c_{nk}$  is coupling constant. The model is symmetric with respect to an exchange of system  $\leftrightarrow$  bath if  $V(Q)$  is the harmonic potential. From Eqs.

(1)-(4), we obtain  $2(N_S + N_B)$  first-order differential equations,

$$\dot{Q}_k = \frac{P_k}{M}, \quad (5)$$

$$\dot{P}_k = -V'(Q_k) - \sum_{n=1}^{N_B} c_{kn}(Q_k - q_n), \quad (6)$$

$$\dot{q}_n = \frac{p_n}{m}, \quad (7)$$

$$\dot{p}_n = -m\omega_n^2 q_n - \sum_{k=1}^{N_S} c_{kn}(q_n - Q_k), \quad (8)$$

which yield

$$M\ddot{Q}_k = -V'(Q_k) - \sum_{n=1}^{N_B} c_{kn}(Q_k - q_n), \quad (9)$$

$$m\ddot{q}_n = -m\omega_n^2 q_n - \sum_{k=1}^{N_S} c_{kn}(q_n - Q_k), \quad (10)$$

with prime ( $'$ ) and dot ( $\dot{\cdot}$ ) denoting derivatives with respect to the argument and time, respectively. It is noted that the second term of Eq. (6) or (9) given by

$$F_k^{(eff)} = - \sum_{n=1}^{N_B} c_{kn}(Q_k - q_n), \quad (11)$$

plays a role of the effective force to the  $k$ th system.

A formal solution of Eq. (10) for  $q_n(t)$  is given by

$$q_n(t) = q_n(0) \cos \tilde{\omega}_n t + \frac{\dot{q}_n(0)}{\tilde{\omega}_n} \sin \tilde{\omega}_n t + \sum_{\ell=1}^{N_S} \frac{c_{\ell n}}{m\tilde{\omega}_n} \int_0^t \sin \tilde{\omega}_n(t-t') Q_\ell(t') dt', \quad (12)$$

with

$$\tilde{\omega}_n^2 = \frac{b_n}{m} + \sum_{k=1}^{N_S} \frac{c_{kn}}{m} = \omega_n^2 + \sum_{k=1}^{N_S} \frac{c_{kn}}{m}. \quad (13)$$

Substituting Eq. (12) to Eq. (9), we obtain the non-Markovian Langevin equation given by

$$\begin{aligned} M\ddot{Q}_k(t) &= -V'(Q_k) - M \sum_{\ell=1}^{N_S} \xi_{k\ell} Q_\ell(t) - \sum_{\ell=1}^{N_S} \int_0^t \gamma_{k\ell}(t-t') \dot{Q}_\ell(t') dt' \\ &- \sum_{\ell=1}^{N_S} \gamma_{k\ell}(t) Q_\ell(0) + \zeta_k(t) \quad (k = 1 \text{ to } N_S), \end{aligned} \quad (14)$$

with

$$M\xi_{k\ell} = \sum_{n=1}^{N_B} \left[ c_{kn}\delta_{k\ell} - \frac{c_{kn}c_{\ell n}}{m\tilde{\omega}_n^2} \right], \quad (15)$$

$$\gamma_{k\ell}(t) = \sum_{n=1}^{N_B} \left( \frac{c_{kn}c_{\ell n}}{m\tilde{\omega}_n^2} \right) \cos \tilde{\omega}_n t, \quad (16)$$

$$\zeta_k(t) = \sum_{n=1}^{N_B} c_{kn} \left[ q_n(0) \cos \tilde{\omega}_n t + \frac{\dot{q}_n(0)}{\tilde{\omega}_n} \sin \tilde{\omega}_n t \right], \quad (17)$$

where  $\xi_{k\ell}$  denotes the additional interaction between  $k$  and  $\ell$ th particles in the system induced by couplings  $\{c_{kn}\}$ ,  $\gamma_{k\ell}(t)$  the memory kernel and  $\zeta_k$  the stochastic force.

If the equipartition relation is realized in initial values of  $q_n(0)$  and  $\dot{q}(0)$ ,

$$\langle m\tilde{\omega}_n^2 q_n(0)^2 \rangle_B = \langle m\dot{q}_n(0)^2 \rangle_B = k_B T, \quad (18)$$

we obtain the fluctuation-dissipation relation:

$$\langle \zeta_k(t)\zeta_k(t') \rangle_B = k_B T \gamma_{kk}(t-t'), \quad (19)$$

where  $\langle \cdot \rangle_B$  stands for the average over variables in the bath.

In the case of  $N_B \rightarrow \infty$ , summations in Eqs. (15)-(17) are replaced by integrals. When the spectral density defined by

$$J(\omega) = \frac{\pi}{2} \sum_n \frac{c_n^2}{m_n \omega_n^2} \delta(\omega - \omega_n), \quad (20)$$

is given by the Ohmic form:  $J(\omega) \propto \omega$  for  $0 \leq \omega < \omega_D$ , the kernel becomes

$$\gamma(t) \propto \frac{\sin \omega_D t}{\pi t} \propto \delta(t), \quad (21)$$

which leads to the Markovian Langevin equation.

In the case of  $N_S = 1$ , we obtain  $\xi$  and  $\gamma$  in Eqs. (15) and (16) where the subscripts  $k$  and  $\ell$  are dropped (*e.g.*,  $c_{kn} = c_n$ ),

$$M\xi(t) = \sum_{n=1}^{N_B} c_n \left( 1 - \frac{c_n}{m\tilde{\omega}_n^2} \right), \quad (22)$$

$$\gamma(t) = \sum_{n=1}^{N_B} \left( \frac{c_n^2}{m\tilde{\omega}_n^2} \right) \cos \tilde{\omega}_n t. \quad (23)$$

The additional interaction vanishes ( $\xi = 0$ ) if we choose  $c_n = m\tilde{\omega}_n^2$  in Eq. (22).

In the case of  $N_S \neq 1$ , however, it is impossible to choose  $\{c_{kn}\}$  such that  $\xi_{k\ell} = 0$  is realized for all pairs of  $(k, \ell)$  in Eq. (15). Then  $Q_k$  is inevitably coupled to  $Q_\ell$  for  $\ell \neq k$  with the superexchange-type interaction of antiferromagnets:  $-\sum_n c_{kn}c_{\ell n}/m\tilde{\omega}_n^2$  in Eq. (15).

### III. MODEL CALCULATIONS FOR DOUBLE-WELL SYSTEMS

#### A. Calculation methods

We consider a system with the double-well potential

$$V(Q) = \left(\frac{\Delta}{Q_0^4}\right)(Q^2 - Q_0^2)^2, \quad (24)$$

which has the stable minima of  $V(\pm Q_0) = 0$  at  $Q = \pm Q_0$  and locally unstable maximum of  $V(0) = \Delta$  at  $Q = 0$  with the barrier height  $\Delta$ . We have adopted  $Q_0 = 1.0$  and  $\Delta = 1.0$  in our DSs.

It is easier to solve  $2(N_S + N_B)$  first-order differential equations given by Eqs. (5)-(8) than to solve the  $N_S$  Langevin equations given by Eqs. (14)-(17) although the latter provides us with clearer physical insight than the former. In order to study the  $N_S$  and  $N_B$  dependences of various physical quantities, we have assumed that the coupling  $c_{kn}$  is given by [10, 24]

$$c_{kn} = \frac{c_o}{N_S N_B}, \quad (25)$$

because the interaction term includes summations of  $\sum_{k=1}^{N_S}$  and  $\sum_{n=1}^{N_B}$  in Eq. (4). It is noted that with our choice of  $c_{kn}$ , the interaction contribution is finite even in the thermodynamical limit of  $N_B \rightarrow \infty$  because the summation over  $n$  runs from 1 to  $N_B$  in Eq. (4). DSs of Eqs. (5)-(8) have been performed with the use of the fourth-order Runge-Kutta method with the time step of 0.01. We have adopted  $k_B = 1.0$ ,  $M = m = 1.0$ ,  $c_o = 1.0$ , and  $\omega_n = 1.0$  otherwise noticed.

We consider energies per particle  $u_\eta(t)$  in the system ( $\eta=S$ ) and the bath ( $\eta=B$ ) which are assume to be given by

$$u_S = \frac{1}{N_S} \sum_{k=1}^{N_S} \left[ \frac{P_k^2}{2M} + V(Q_k) \right], \quad (26)$$

$$u_B = \frac{1}{N_B} \sum_{n=1}^{N_B} \left[ \frac{p_n^2}{2m} + \frac{m\omega_n^2 q_n^2}{2} \right], \quad (27)$$

which is valid for the weak interaction, although a treatment of the finite interaction is ambiguous and controversial [5, 6].

## B. Dynamics of a particle in the $(Q, P)$ phase space

### 1. Effect of $c_o$

First we consider an isolated double-well system ( $N_S = 1$  and  $c_o = 0.0$ ). Figure 1 shows the phase-space trajectories in the  $(Q, P)$  phase space for this system with six different initial system energies  $E_{S_o}$ . For  $E_{S_o} = 0.0$ , the system has two stable fixed points at  $(Q, P) = (\pm 1.0, 0.0)$ , and for  $E_{S_o} = \Delta = 1.0$  it has one unstable fixed point at  $(Q, P) = (0.0, 0.0)$ . In the case of  $0.0 < E_{S_o} < 1.0$ , the trajectory is restricted in the region of  $Q > 0.0$  (or  $Q < 0.0$ ). In contrast in the case of  $E_{S_o} > 1.0$ , trajectory may visit both regions of  $Q > 0.0$  and  $Q < 0.0$ . The case of  $E_{S_o} = 1.0$  is critical between the two cases.

Next the double-well system is coupled to a bath. In our DSs, we have assumed that system and bath are decoupled at  $t < 0$  where they are in equilibrium states with  $E_{S_o} = T$ , the temperature  $T$  being defined by  $T = u_B$ . We have chosen initial values of  $Q(0) = 1.0$  and  $P(0) = \sqrt{2M[E_{S_o} - V(Q(0))]}$  for a given initial system energy  $E_{S_o}$ . Initial conditions for  $q_n(0)$  and  $p_n(0)$  are given by random Gaussian variables with zero means and variance proportional to  $T$  [Eq. (18)] [10]. Results to be reported in this subsection have been obtained by single runs for  $t = 0$  to 1000.

Figures 2(a) and 2(b) show a strobe plot in the  $(Q, P)$  phase space (with a time interval of 1.0) and the time-dependence of  $Q(t)$ , respectively, for  $E_{S_o} = 1.0$ ,  $N_S = 1$ ,  $N_B = 100$  and  $c_o = 0.2$ . The trajectory starting from  $Q(0) = 1.0$  goes to the negative- $Q$  region because a particle may go over the potential barrier with a help of a force (noise) originating from bath given by Eq. (11). The system energy fluctuates as shown in Fig. 2(c), whose distribution is plotted in Fig. 2(d).

Results in Fig. 2 are regular. In contrast, when a coupling strength is increased to  $c_o = 1.0$ , the system becomes chaotic as shown in Figs. 3(a) and 3(b) where a strobe plot in the  $(Q, P)$  phase space and the time-dependence of  $Q(t)$  are plotted, respectively. This is essentially the force-induced chaos in classical double-well system [23]: although an external force is not applied to our system, a force arising from a coupling with bath given by Eq. (11) plays a role of an effective external force for the system. Figures 3(c) and 3(d) show that in the case of  $c_o = 1.0$ ,  $u_S$  has more appreciable temporal fluctuations with a wider energy distribution in  $f_S(u)$  than in the case of  $c_o = 0.2$ . Although system energies fluctuate, they

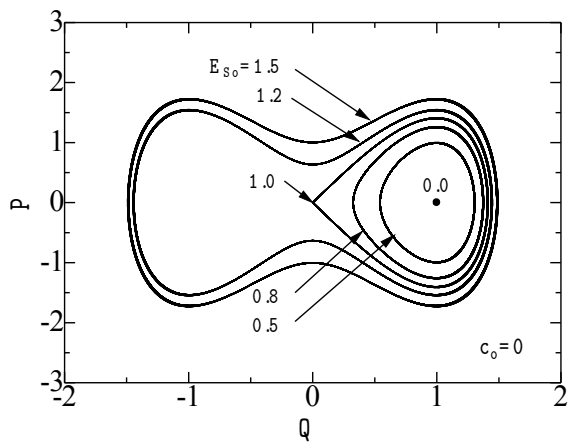


FIG. 1: Plot of phase-space trajectories for a particle in an isolated double-well system ( $c_o = 0.0$ ). Trajectories are plotted for energies of  $E_{S_o}/\Delta = 0.0, 0.5, 0.8, 1.0, 1.2$  and  $1.5$ .

are not dissipative at  $0.0 \leq t < 1000.0$  in DSs both for  $c_o = 0.2$  and  $c_o = 1.0$  with  $N_B = 100$ .

## 2. Effect of $\omega_n$ distributions

We have so far assumed  $\omega_n = 1.0$  in the bath, which is now changed. Figures 4(a) and 4(c) show strobe plots for  $\omega_n = 0.5$  and  $2.0$ , respectively, which are regular and which are different from a chaotic result for  $\omega_n = 1.0$  shown in Fig. 4(b). When we adopt  $\{\omega_n\}$  which is randomly distributed in  $[0.5, 2.0]$ , a motion of a system particle becomes chaotic as shown



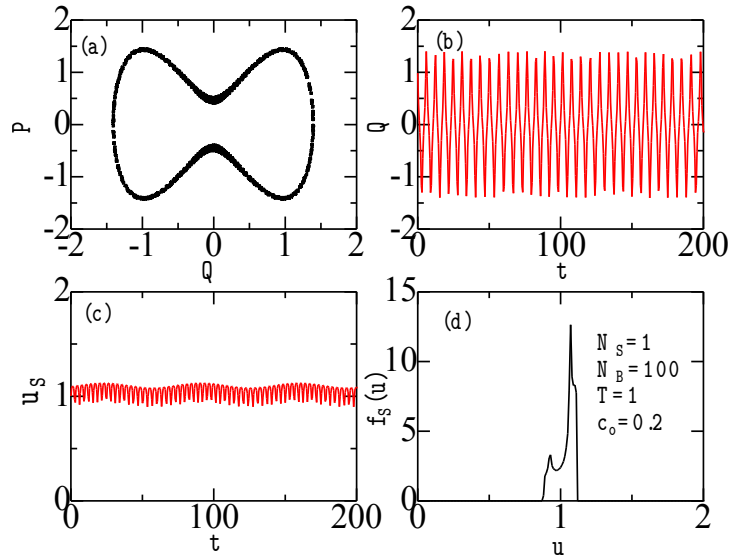


FIG. 2: (Color online) (a) Strobe plot in the  $(Q, P)$  phase space (with a time interval of 1.0), (b)  $Q(t)$ , (c)  $u_S(t)$ , and (d) the system energy distribution  $f_S(u)$  obtained by a single run for  $E_{S_o} = 1.0$ ,  $N_S = 1$ ,  $N_B = 100$ ,  $T = 1.0$  and  $c_o = 0.2$ .

in Fig. 4(d). This is because contributions from  $\omega_n \sim 1.0$  among  $[0.5, 2.0]$  induce chaotic behavior.

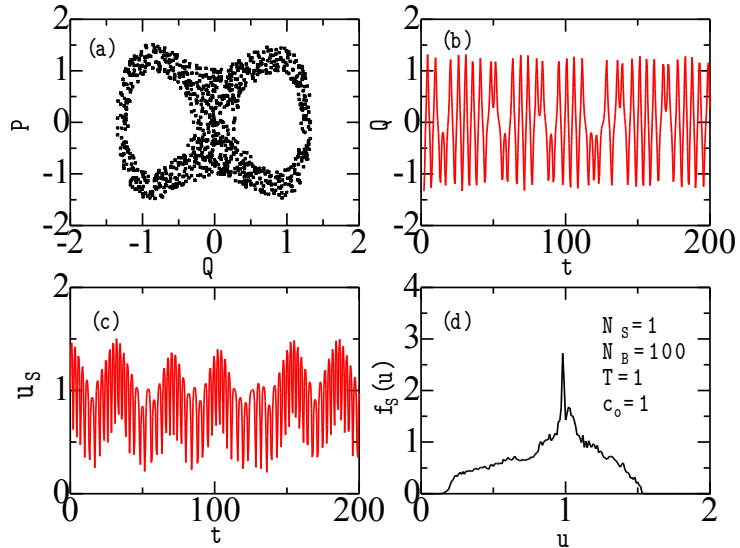


FIG. 3: (Color online) (a) Strobe plot in the  $(Q, P)$  phase space, (b)  $Q(t)$ , (c)  $u_S(t)$ , and (d) the system energy distribution  $f_S(u)$  obtained by a single run for  $E_{S_o} = 1.0$ ,  $N_S = 1$ ,  $N_B = 100$ ,  $T = 1.0$  and  $c_o = 1.0$ .

### 3. Effect of $N_B$

We have repeated calculations by changing  $N_B$ , whose results are plotted in Figs. 5(a)-5(d). Figures 5(a), 5(b) and 5(c) show that chaotic behaviors for  $N_B = 2$  and  $N_B = 10$  are

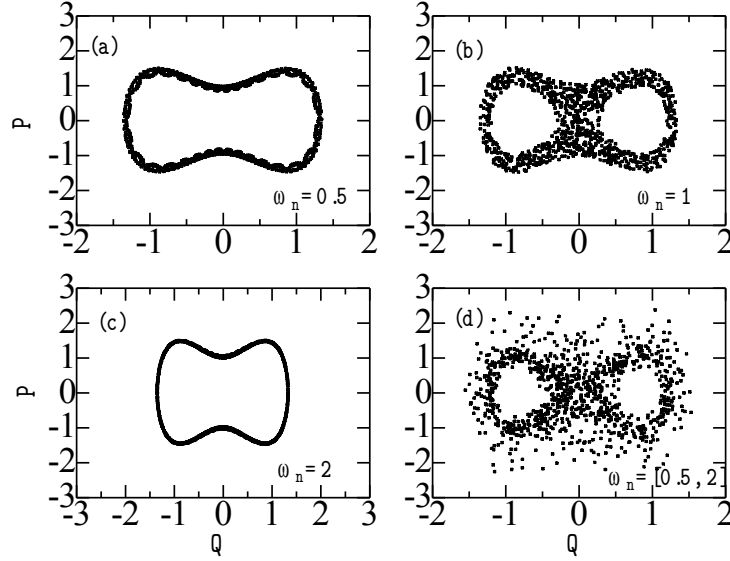


FIG. 4: Strobe plots in the  $(Q, P)$  phase space for various distribution of  $\{\omega_n\}$ : (a)  $\omega_n = 0.5$ , (b)  $\omega_n = 1.0$ , (c)  $\omega_n = 2.0$  and (d)  $\omega_n \in [0.5, 2.0]$  obtained by single runs with  $E_{S_0} = 1.0$ ,  $N_S = 1$ ,  $N_B = 100$ ,  $T = 1.0$  and  $c_o = 1.0$ .

more significant than that for  $N_B = 100$ . On the contrary, chaotic behavior is not realized for  $N_B = 1000$  in Fig. 5(d), which is consistent with the fact that chaos has not been reported for the double-well system subjected to infinite bath.

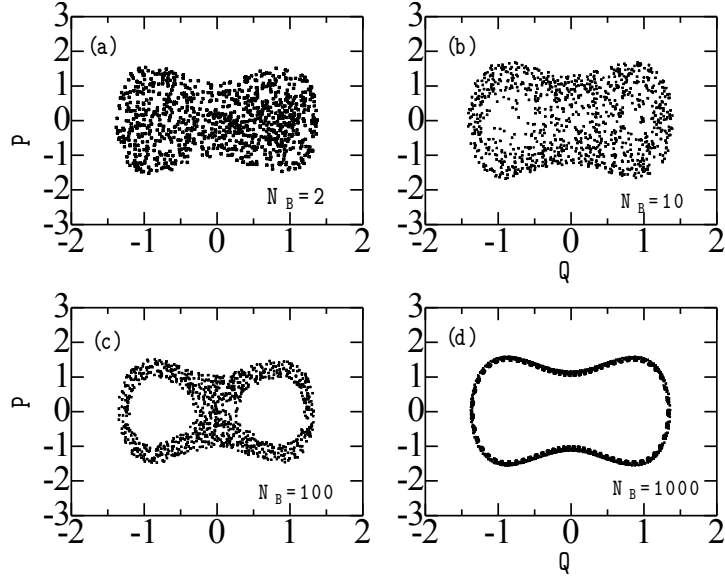


FIG. 5: Strobe plots in the  $(Q, P)$  phase space for various  $N_B$ : (a)  $N_B = 2$ , (b)  $N_B = 10$ , (c)  $N_B = 100$  and (d)  $N_B = 1000$  with  $E_{S_o} = 1.0$ ,  $N_S = 1$ ,  $T = 1.0$  and  $c_o = 1.0$ .

#### 4. Effect of initial system energy $E_{S_o}$

Next we change the initial system energy of  $E_{S_o}$ . Figures 6(a)-(d) show strobe plots in the  $(Q, P)$  phase space for various  $E_{S_o}$  with  $N_S = 1$ ,  $N_B = 100$ ,  $T = 1.0$  and  $c_o = 1.0$ . Figure 6(a) shows that for  $E_{S_o} = 0.5$ , the regular trajectory starting from  $Q = 1.0$  remains

in the positive- $Q$  region because a particle cannot go over the potential barrier of  $\Delta = 1.0$ . For  $E_{S_o} = 0.8$ , chaotic trajectories may go to the negative- $Q$  region with a help of force from bath [Eq. 11]. Figure 6(d) shows that when  $E_{S_o}$  is too large compared to  $\Delta$  ( $E_{S_o}/\Delta = 1.2$ ), the trajectory again becomes regular, going between positive- and negative- $Q$  regions.

Figure 7 shows the system energy distribution  $f_S(u)$  for various  $E_{S_o}$ .  $f_S(u)$  moves upward as  $E_{S_o}$  is increased. It is noted that peak positions of  $f_S(u)$  for  $E_{S_o} = 0.5 - 1.0$  locate at  $u \simeq 1.0$  while that for  $E_{S_o} = 1.2$  locates at  $u \simeq 1.35$ .

### C. Stationary energy probability distributions

In this subsection, we will study stationary energy probability distributions of system and bath which are averaged over  $N_r$  ( $=10\ 000$ ) runs starting from different initial conditions. Assuming that the system and bath are in the equilibrium states with  $T = u_B = u_S$  at  $t < 0.0$ , we first generate exponential derivatives of initial system energies  $\{E_j\}$ :  $p(E_j) \propto \exp(-\beta E_j)$  ( $j = 1$  to  $N_S N_r$ ) for our DSs where  $\beta = 1/k_B T$ . A pair of initial values of  $Q_j(0)$  and  $P_j(0)$  for a given  $E_j$  is randomly chosen such that they meet the condition given by  $E_j = P_j(0)^2/2M + V(Q_j(0))$ . The procedure for choosing initial values of  $q_n(0)$  and  $p_n(0)$  is the same as that adopted in the preceding subsection [10]. We have discarded results for  $t < 200$  in our DSs performed for  $t = 0$  to 1000.

Before discussing cases where  $N_S$  and  $N_B$  may be greater than unity, we first study a pedagogical simple case of  $N_S = N_B = 1$ : a particle with double-well potential is subjected to a single harmonic oscillator. Double-chain curves in Fig. 8(a) and 8(b) show energy distributions of the system [ $f_S(u)$ ] and bath [ $f_B(u)$ ], respectively, with  $c_o = 0.0$ , where  $u = u_S$  ( $u = u_B$ ) for the system (bath). Both  $f_S(u_S)$  and  $f_B(u_B)$  follow the exponential distribution because the assumed initial equilibrium states of decoupled system and bath persist at  $t \geq 0.0$ . When they are coupled by a weak coupling of  $c_o = 0.1$  at  $t \geq 0.0$ ,  $f_S(u)$  and  $f_B(u)$  almost remain exponential distributions except for that  $f_S(u)$  has a small peak at  $u = 1.0$ , as shown by dashed curve in Fig. 8(a). This peak has been realized in Figs. 2(d) and 3(d). It is due to the presence of a potential barrier with  $\Delta = 1.0$  in double-well potential because the peak at  $u = 1.0$  in  $f_S(u)$  is realized even when  $T \neq 1.0$ , as will be discussed later in 4. *Effect of  $T$*  (Fig. 12). This peak is developed for stronger couplings of  $c_o = 1.0$  and 2.0, for which magnitudes of  $f_S(u)$  at small  $u$  are decreased, as shown by solid

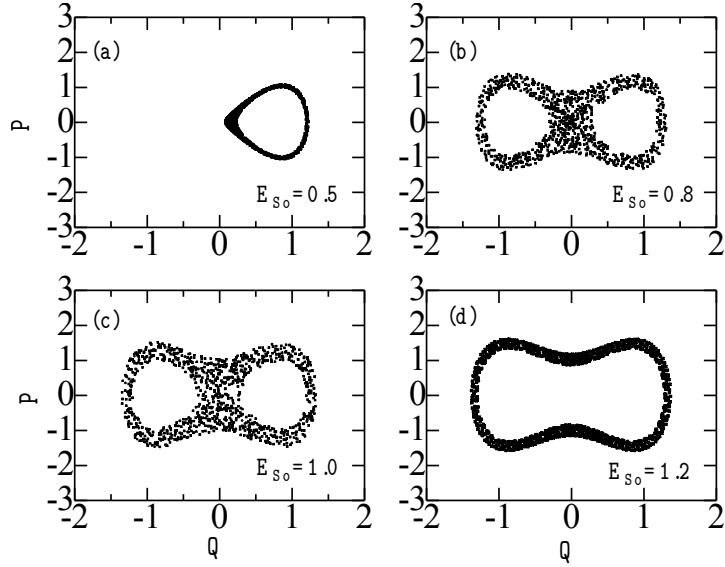


FIG. 6: Strobe plots in the  $(Q, P)$  phase space for various  $E_{S_0}$ : (a)  $E_{S_0} = 0.5$ , (b)  $E_{S_0} = 0.8$  (c)  $E_{S_0} = 1.0$  and  $E_{S_0} = 1.2$  with  $N_S = 1$ ,  $N_B = 100$ ,  $T = 1.0$  and  $c_o = 1.0$ .

and chain curves in Figs. 8(a) and 8(b).

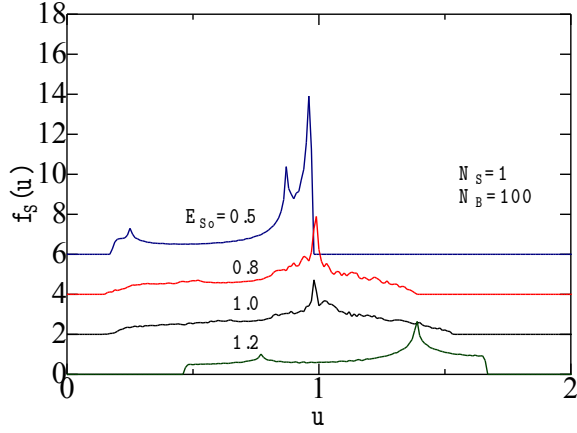


FIG. 7: (Color online) System energy distributions  $f_S(u)$  for  $E_{S_0} = 0.5, 0.8, 1.0$  and  $1.2$  with  $N_S = 1, N_B = 100, T = 1.0$  and  $c_o = 1.0$ , curves being successively shifted upward by two for clarity of figures.

### 1. Effect of $c_o$

We change the coupling strength of  $c_o$ . Figures 9(a) and 9(b) show  $f_S(u)$  and  $f_B(u)$ , respectively, for  $c_o = 0.2, 1.0, 5.0$  and  $10.0$  with  $N_S = 1, N_B = 100$  and  $T = 1.0$ .  $f_S(u)$  for  $c_o = 0.2$  nearly follows the exponential distribution. When  $c_o$  becomes larger, magnitudes of  $f_S(u)$  at  $u < 1.0$  are decreased while that at  $u > 1.0$  is increased. In particular, the magnitude of  $f_S(0)$  is more decreased for larger  $c_o$ .

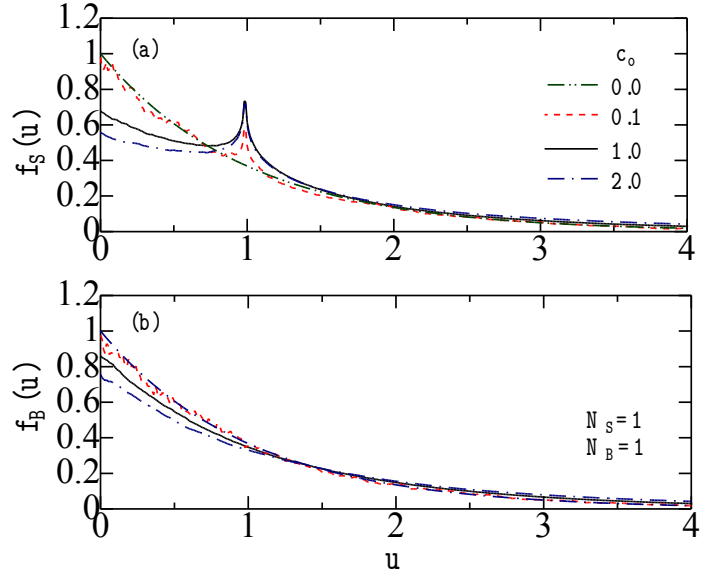


FIG. 8: (Color online) Stationary distributions of (a)  $f_S(u)$  and (b)  $f_B(u)$  for various  $c_o$ :  $c_o = 0.0$  (double-chain curves), 0.1 (dashed curves), 1.0 (solid curves) and 2.0 (chain curves) obtained by 10 000 runs with  $N_S = N_B = 1$  and  $T = 1.0$ .

## 2. Effect of $\omega_n$ distributions

Although we have assumed  $\omega_n = 1.0$  in both oscillators, we will examine the effect of their distribution, taking into account two kinds of random distributions given by  $\omega_n \in [0.5, 2.0]$



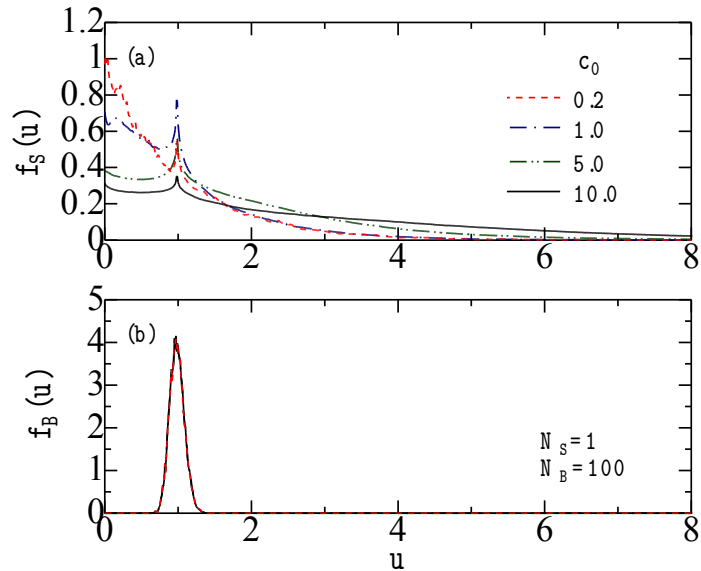


FIG. 9: (Color online) Stationary distributions of (a)  $f_S(u)$  and (b)  $f_B(u)$  for various  $c_0$ :  $c_0 = 0.2$  (dashed curves), 1.0 (chain curves), 5.0 (double-chain curves) and 10.0 (solid curves) with  $N_S = 1$ ,  $N_B = 100$  and  $T = 1.0$ .

and  $\omega_n \in [2.0, 3.0]$ . From calculated results shown in Figs. 10(a) and 10(b), we note that  $f_S(u)$  and  $f_B(u)$  are not much sensitive to the distribution of  $\{\omega_n\}$  in accordance with our previous calculation for harmonic oscillator system [10, 25]. This conclusion, however, might

not be applied to the case of infinite bath where distribution of  $\{\omega_n\}$  becomes continuous distribution. Ref. [8] reported that the relative position between oscillating frequency ranges of system and bath is very important for a thermalization of the harmonic oscillator system subjected to finite bath.

### 3. Effect of $N_B$

We have calculated  $f_S(u)$  and  $f_B(u)$ , changing  $N_B$  but with fixed  $N_S = 1$ , whose results are shown in Figs. 11(a) and 11(b). For larger  $N_B$ , the width of  $f_B(u)$  becomes narrower as expected. However, shapes of  $f_S(u)$  are nearly unchanged for all cases of  $N_B = 1, 10, 100$  and 1000.

### 4. Effect of $T$

We change the temperature of the bath. Figures 12(a) and 12(b) show  $f_S(u)$  and  $f_B(u)$ , respectively, for  $T = 0.5, 1.0$  and  $1.5$  with  $N_S = 1, N_B = 100$  and  $c_o = 1.0$ . When  $T$  is decreased (increased), positions of  $f_B(u)$  move to lower (higher) energy such that mean values of  $u_B$  correspond to  $T$ . For a lower temperature of  $T = 0.5$ , magnitude of  $f_S(u)$  at  $u < 1.0$  is increased while that at  $u > 1.0$  is decreased. The reverse is realized for higher temperature of  $T = 1.5$ . We should note that the peak position in  $f_S(u)$  at  $u = 1.0$  is not changed even if  $T$  is changed because this peak is related to the barrier with  $\Delta = 1.0$  of the double-well potential.

### 5. Effect of $N_S$

Although  $N_S = 1$  has been adopted so far, we will change  $N_s$  to investigate its effects on stationary energy distributions. Figure 13(a) shows  $f_S(u)$  for  $N_S = 1, 2, 5$  and 10.  $f_S(u)$  for  $N_S = 1$  shows an exponential-like distribution with  $f_S(0) \neq 0$  at  $u = 0.0$ . In contrast,  $f_S(u)$  vanishes at  $u = 0.0$  for  $N_S = 2, 5$  and 10. Figure 13(a) shows that shapes of  $f_S(u)$  much depend on  $N_S$  while those of  $f_B(u)$  are almost unchanged in Fig. 13(b).

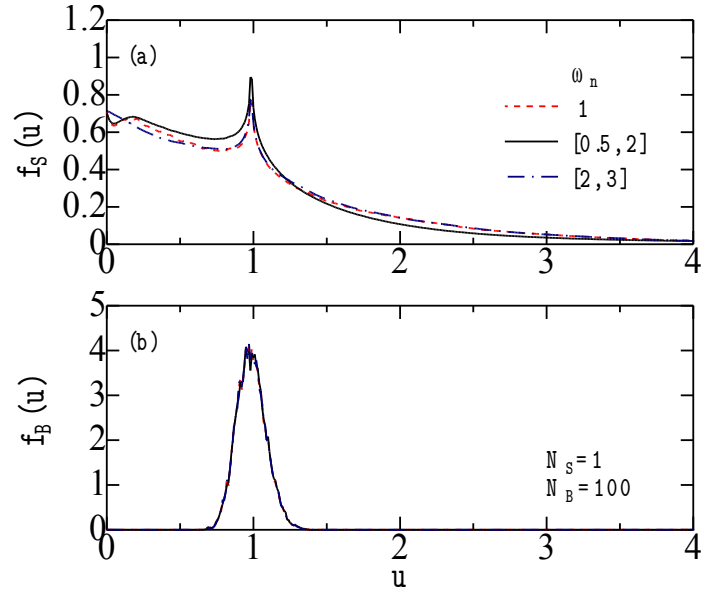


FIG. 10: (Color online) Stationary distributions of (a)  $f_S(u)$  and (b)  $f_B(u)$  for various distributions of  $\{\omega_n\}$ :  $\omega = 1.0$  (dashed curves),  $\omega_n \in [0.5, 2.0]$  (solid curves) and  $\omega_n \in [2.0, 3.0]$  (chain curves) with  $N_S = 1$ ,  $N_B = 100$ ,  $T = 1.0$  and  $c_o = 1.0$ .

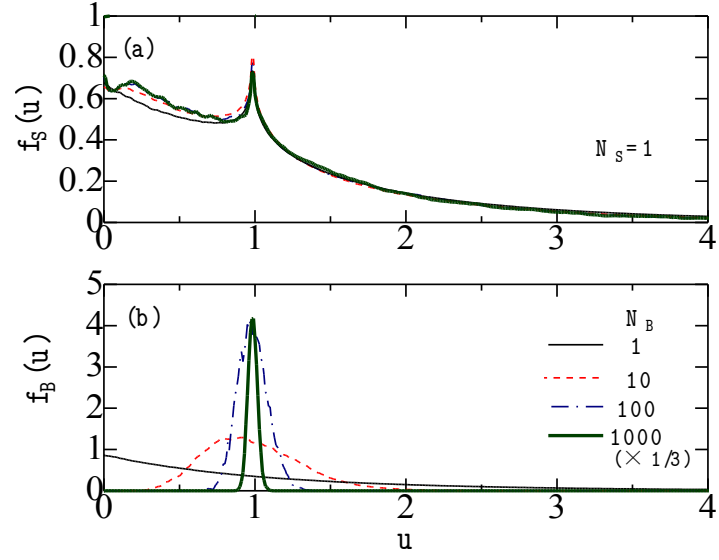


FIG. 11: (Color online) Stationary distributions of (a)  $f_S(u)$  and (b)  $f_B(u)$  for various  $N_B$ :  $N_B = 1$  (solid curves), 10 (dashed curves), 100 (chain curves) and 1000 (bold solid curves) with  $N_S = 1$ ,  $T = 1.0$  and  $c_o = 1.0$ .  $f_B(u)$  for  $N_B = 1000$  is multiplied by a factor of  $1/3$ .

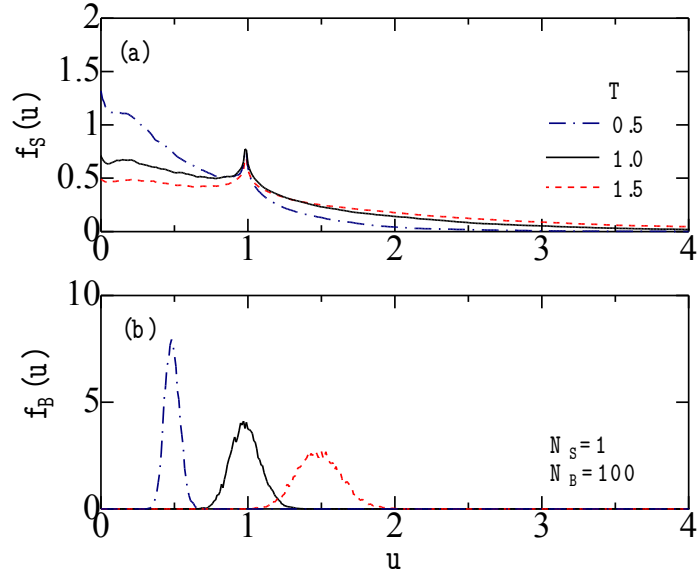


FIG. 12: (Color online) Stationary distributions of (a)  $f_S(u)$  and (b)  $f_B(u)$  for various  $T$ :  $T = 0.5$  (chain curves), 1.0 (solid curves) and 1.5 (dashed curves) with  $N_S = 1$ ,  $N_B = 100$  and  $c_o = 1.0$ .

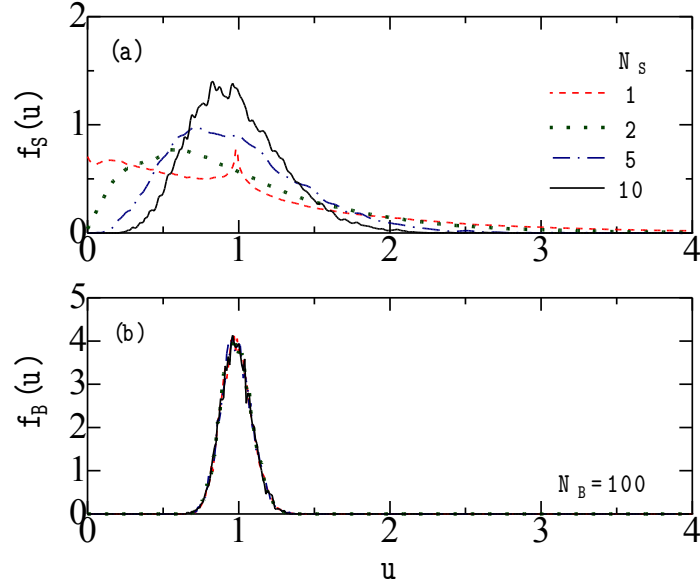


FIG. 13: (Color online) Stationary distributions of (a)  $f_S(u)$  and (b)  $f_B(u)$  for various  $N_S$ :  $N_S = 1$  (dashed curves), 2 (dotted curves), 5 (chain curves) and 10 (solid curves) with  $N_B = 100$ ,  $T = 1.0$  and  $c_o = 1.0$ .

## IV. DISCUSSION

### A. Analysis of stationary energy distributions

Our DSs in the preceding section have shown that  $f_S(u)$  depends mainly on  $N_S$ ,  $c_o$  and  $T$  while  $f_B(u)$  depends mostly on  $N_B$  and  $T$  for  $N_S \ll N_B$ . We will try to analyze  $f_S(u)$  and  $f_B(u)$  in this subsection. It is well known that when variables of  $x_i$  ( $i = 1 - N$ ) are independent and follow the exponential distributions with the same mean, the distribution of its sum:  $X = \sum_i x_i$  is given by the  $\Gamma$  distribution. Then for an uncoupled system ( $c_o = 0.0$ ),  $f_S(u)$  and  $f_B(u)$  are expressed by the  $\Gamma$  distribution  $g(u)$  given by [10]

$$f_\eta(u) = \frac{1}{Z_\eta} u^{a_\eta-1} e^{-b_\eta u} \equiv g(u; a_\eta, b_\eta), \quad (28)$$

with

$$a_\eta = N_\eta, \quad b_\eta = N_\eta \beta, \quad (29)$$

$$Z_\eta = \frac{\Gamma(a_\eta)}{b_\eta^{a_\eta}}, \quad (30)$$

where  $\eta = S$  and  $B$  for a system and bath, respectively, and  $\Gamma(x)$  is the gamma function. In the limit of  $N_S = 1$ , the  $\Gamma$  distribution reduces to the exponential distribution. Mean ( $\mu_\eta$ ) and variance ( $\sigma_\eta^2$ ) of the  $\Gamma$  distribution are given by

$$\mu_\eta = \frac{a_\eta}{b_\eta}, \quad \sigma_\eta^2 = \frac{a_\eta}{b_\eta^2}, \quad (31)$$

from which  $a_\eta$  and  $b_\eta$  are expressed in terms of  $\mu_\eta$  and  $\sigma_\eta$

$$a_\eta = \frac{\mu_\eta^2}{\sigma_\eta^2}, \quad b_\eta = \frac{\mu_\eta}{\sigma_\eta^2}. \quad (32)$$

We have tried to evaluate  $f_S(u)$  and  $f_B(u)$  for the coupled system ( $c_o \neq 0.0$ ) as follows: From mean ( $\mu_\eta$ ) and root-mean-square (RMS) ( $\sigma_\eta$ ) calculated by DSs,  $a_\eta$  and  $b_\eta$  are determined by Eq. (32), with which we obtain the  $\Gamma$  distributions for  $f_S(u)$  and  $f_B(u)$ . Filled and open squares in Fig. 14 show  $\mu_B$  and  $\sigma_B$ , respectively, as a function of  $N_S$ . We obtain  $\mu_B = 1.0$  and  $\sigma_B = 0.1$  nearly independently of  $N_S$ , which yield  $a_B = b_B = 100.0$  in agreement with Eq. (29). Filled and open triangles in Fig. 14 express the  $N_S$  dependence of  $\mu_S$  and  $\sigma_S$  obtained by DSs with  $c_o = 1.0$ ,  $N_B = 100$  and  $T = 1.0$ . Calculated mean and RMS values of  $(\mu_S, \sigma_S)$  are (1.07, 0.98), (0.99, 0.70), (0.99, 0.44) and (0.99, 0.319) for  $N_S = 1, 2, 5$

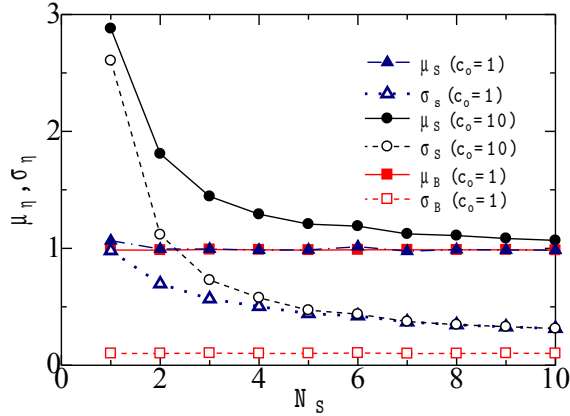


FIG. 14: (Color online)  $N_S$  dependences of  $\mu_\eta$  and  $\sigma_\eta$  of system ( $\eta = S$ ) and bath ( $\eta = B$ ) with  $N_B = 100$  and  $T = 1.0$ : filled (open) triangles denote  $\mu_S$  ( $\sigma_S$ ) with  $c_o = 1.0$ : filled (open) circles express  $\mu_S$  ( $\sigma_S$ ) with  $c_o = 10.0$ : filled (open) squares show  $\mu_B$  ( $\sigma_B$ ) with  $c_o = 1.0$ .

and 10, respectively, for which Eq. (32) yields  $(a_S, b_S) = (1.18, 1.11), (2.04, 2.05), (4.50, 5.06)$  and  $(9.82, 9.97)$ . These values of  $a_S$  and  $b_S$  are not so different from  $N_S$  and  $N_S\beta$  given by Eq. (29). We have employed the  $\Gamma$  distribution with these parameters  $a_S$  and  $b_S$  for our analysis of  $f_S(u)$  having been shown in Fig. 13(a). Dashed curves in Figs. 15(a)-(d) express calculated  $\Gamma$  distributions, which are in fairly good agreement with  $f_S(u)$  plotted by solid curves, except for  $N_S = 1$  for which  $g(0) = 0.0$  because  $a_S = 1.18 > 1.0$  while  $f_S(0) \neq 0.0$ .

Similar analysis has been made for another result obtained with a larger  $c_o = 10.0$  for



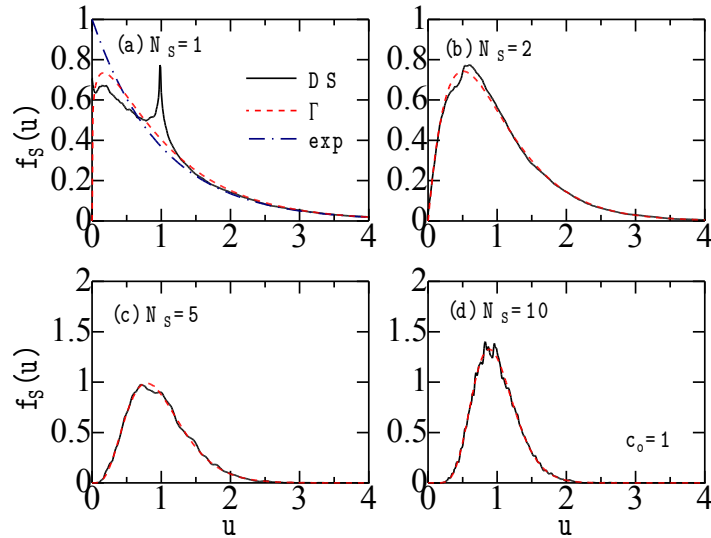


FIG. 15: (Color online)  $u$  dependences of  $f_S(u)$  for (a)  $N_S = 1$ , (b)  $N_S = 2$ , (c)  $N_S = 5$  and (d)  $N_S = 10$  with  $T = 1.0$ ,  $c_o = 1.0$  and  $N_B = 100$  obtained by DSs (solid curves): dashed and chain curves express  $\Gamma$  and exponential distributions, respectively (see text).

$N_B = 100$  and  $T = 1.0$ .  $N_S$ -dependences of calculated  $\mu_S$  and  $\sigma_S$  are plotted by filled and open circles, respectively, in Fig. 14. Calculated  $(\mu_S, \sigma_S)$  are  $(2.88, 2.61)$ ,  $(1.81, 1.12)$ ,  $(1.21, 0.47)$  and  $(1.07, 0.31)$  for  $N_S = 1, 2, 5$  and  $10$ , respectively, which lead to  $(a_S, b_S) =$

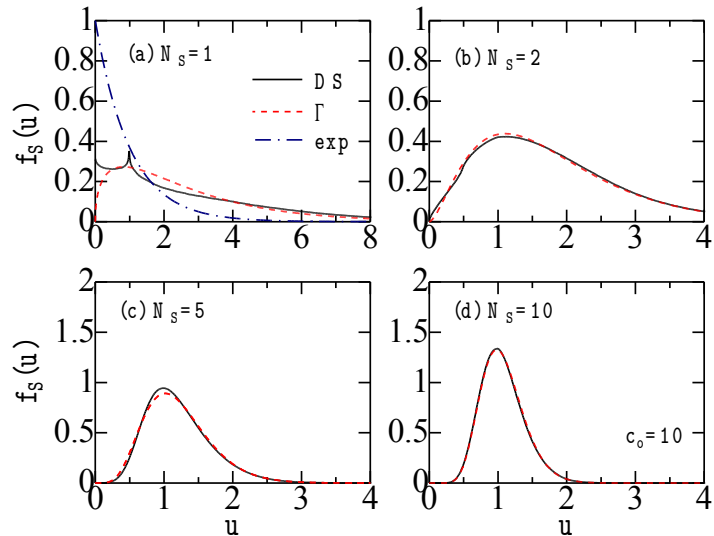


FIG. 16: (Color online)  $u$  dependences of  $f_S(u)$  for (a)  $N_S = 1$ , (b)  $N_S = 2$ , (c)  $N_S = 5$  and (d)  $N_S = 10$  with  $T = 1.0$ ,  $c_o = 10.0$  and  $N_B = 100$  obtained by DSs (solid curves): dashed and chain curves express  $\Gamma$  and exponential distributions, respectively (see text).

(1.22, 0.42), (2.62, 1.45), (6.57, 5.44) and (11.54, 10.81) by Eq. (32). Obtained  $a_S$  and  $b_S$  are rather different from  $N_S$  and  $N_S\beta$  given by Eq. (29). Dashed curves in Figs. 16(a)-(d) show  $\Gamma$  distributions with these parameters, which may approximately explain  $f_S(u)$  obtained by

DSs in the *phenomenologically* sense, except for  $N_S = 1$  for which  $g(0) = 0.0$  but  $f_S(0) \neq 0.0$ .

We note in Fig. 15(a) or 16(a) that an agreement between  $g(u)$  and  $f_S(u)$  with  $N_S = 1$  is not satisfactory. We have tried to obtain a better fit between them, by using the  $q$ - $\Gamma$  distribution  $g_q(u)$  given by [10]

$$g_q(u) = \frac{1}{Z_q} u^{a-1} e_q^{-bu}, \quad (33)$$

with

$$e_q^x = [1 + (1 - q)x]_+^{1/(1-q)}, \quad (34)$$

where  $[y]_+ = \max(y, 0)$  and  $Z_q$  is the normalization factor. Note that  $g_q(u)$  reduces to the  $\Gamma$  distribution in the limit of  $q \rightarrow 1.0$ . Although the  $q$ - $\Gamma$  distribution was useful for  $f_S(u)$  of harmonic-oscillator systems subjected to finite bath [10], it does not work for  $f_S(u)$  of double-well systems. This difference may be understood from a comparison between  $f_S(u)$  for  $N_S = 1$  of a double-well system shown in Fig. 15(a) [or 16(a)] and its counterpart of a harmonic oscillator system shown in Fig. 9(a) of Ref. [10]. Although the latter shows an exponential-like behavior with a monotonous decrease with increasing  $u$ , the former with a characteristic peak at  $u = 1.0$  cannot be expressed by either the exponential,  $\Gamma$ , or  $q$ - $\Gamma$  distribution.

## B. Analysis of stationary position distributions

We have studied also the  $N_S$  dependence of stationary position distributions of  $p(Q)$  and  $P(\bar{Q})$ , where  $Q$  denotes the position of a particle in the system and  $\bar{Q}$  expresses the averaged position given by

$$\bar{Q} = \frac{1}{N_S} \sum_{k=1}^{N_S} Q_k. \quad (35)$$

Figures 17(a) and 17(b) show  $p(Q)$  and  $P(\bar{Q})$ , respectively, obtained by DSs for various  $N_S$  with  $N_B = 100$ ,  $T = 1.0$  and  $c_o = 1.0$ . For  $N_S = 1$ , we obtain  $p(Q) = P(\bar{Q})$  with the characteristic double-peaked structure. We note, however, that  $P(\bar{Q})$  is different from  $p(Q)$  for  $N_S > 1$  for which  $P(\bar{Q})$  has a single-peaked structure despite the double-peaked  $p(Q)$ . This is easily understood as follows: For example, in the case of  $N_S = 2$ , two particles in

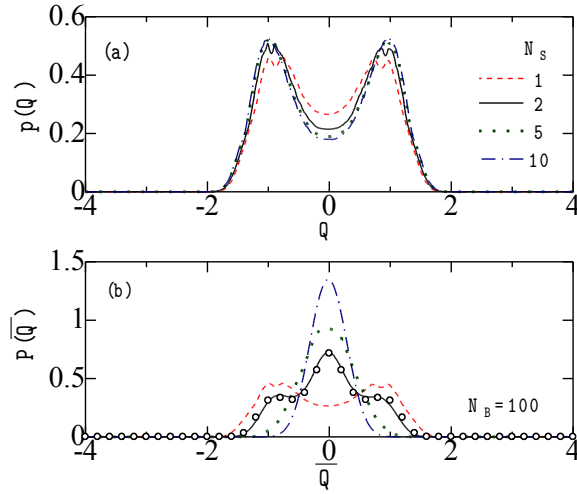


FIG. 17: (Color online) Stationary distributions of (a)  $p(Q)$  as a function of particle position  $Q$  and (b)  $P(\bar{Q})$  as a function of the averaged position  $\bar{Q}$  for various  $N_S$ :  $N_S = 1$  (dashed curve), 2 (solid curve), 5 (dotted curve) and 10 (chain curve) with  $N_B = 100$ ,  $T = 1.0$  and  $c_o = 1.0$ . Open circles in (b) express an analytical result obtained by Eq. (36) with  $N_S = 2$ .

the system mainly locate at  $Q_k = 1.0$  or  $Q_k = -1.0$  ( $k = 1, 2$ ) which yields the double-peaked distribution of  $f_S(Q)$ . However, the averaged position of  $\bar{Q} = (Q_1 + Q_2)/2$  will be dominantly  $\bar{Q} = 0.0$ , which leads to a single-peaked  $P(\bar{Q})$ . The situation is the same also for  $N_S > 2$ .

Theoretically  $P(\bar{Q})$  may be expressed by

$$P(\bar{Q}) = \int \cdots \int \prod_{k=1}^{N_S} dQ_k \exp[-\beta V(Q_k)] \delta \left( \bar{Q} - N_S^{-1} \sum_{k=1}^{N_S} Q_k \right). \quad (36)$$

$P(\bar{Q})$  numerically evaluated for  $N_S = 2$  is plotted by open circles in Fig. 17 which are in good agreement with the solid curve expressing  $P(\bar{Q})$  obtained by DS. It is impossibly difficult to numerically evaluate Eq. (36) for  $N_S \geq 3$ . In the limit of  $N_S \rightarrow \infty$ ,  $P(\bar{Q})$  reduces to the Gaussian distribution according to the central-limit theorem. This trend is realized already in the case of  $N_S = 10$  in Fig. 17(b).

## V. CONCLUDING REMARKS

We have studied the properties of classical double-well systems coupled to finite bath, employing the  $(N_S + N_B)$  model [10] in which  $N_S$ -body system is coupled to  $N_B$ -body bath. Results obtained by DSs have shown the following:

- (i) Chaotic oscillations are induced in the double-well system coupled to finite bath in the absence of external forces for appropriate model parameters of  $c_o$ ,  $N_B$ ,  $T$ ,  $\{\omega_n\}$  and  $E_{S_o}$ ,
- (ii) Among model parameters,  $f_S(u)$  depends mainly on  $N_S$ ,  $c_o$  and  $T$  while  $f_B(u)$  depends on  $N_B$  and  $T$  for  $N_S \ll N_B$ ,
- (iii)  $f_S(u)$  for  $N_S > 1$  obtained by DSs may be phenomenological expressed by the  $\Gamma$  distribution,
- (iv)  $f_S(u)$  for  $N_S = 1$  with  $c_o \neq 0.0$  cannot be described by either the exponential,  $\Gamma$ , or  $q$ - $\Gamma$  distribution, although that with  $c_o = 0.0$  follows the exponential distribution, and
- (v) The dissipation is not realized in the system energy for DSs at  $t = 0 - 1000$  with  $N_S = 1 - 100$  and  $N_B = 10 - 1000$ .

The item (i) is in consistent with chaos in a closed classical double-well system driven by external forces [23], although chaos is induced without external forces in our open classical double-well system. This is somewhat reminiscent of chaos induced by quantum noise in the absence of external force in closed quantum double-well systems [27]. Effects of induced chaos in the item (i) are not apparent in  $f_S(u)$  because  $u$  ( $= u_S$ ) is ensemble averaged over 10 000 runs (realizations) with exponentially distributed initial system energies. Items (ii) and (v) are the same as in the harmonic-oscillator system coupled to finite bath [10]. The item (v) suggests that for the energy dissipation of system, we might need to adopt a much larger

$N_B (\gg 1000)$  [26]. The item (iv) is in contrast to  $f_S(u)$  for  $N_S = 1$  in the open harmonic-oscillator system which may be approximately accounted for by the  $q$ - $\Gamma$  distribution [10]. It would be necessary and interesting to make a quantum extension of our study which is left as our future subject.

### Acknowledgments

This work is partly supported by a Grant-in-Aid for Scientific Research from Ministry of Education, Culture, Sports, Science and Technology of Japan.

- 
- [1] A. O. Caldeira and A. J. Leggett, Phys. Rev. Lett. **46**, 211 (1981).
  - [2] A. O. Caldeira and A. J. Leggett, Ann. Phys. **149**, 374 (1983).
  - [3] V. B. Magalinskii, Sov. Phys. JETP **9**, 1381 (1959).
  - [4] P. Ullersma, Physica **32**, 27 (1966); *ibid.* **32**, 56 (1966); *ibid.* **32**, 74 (1966); *ibid.* **32**, 90 (1966).
  - [5] P. Hanggi, Gert-Ludwig Ingold and P. Talkner, New Journal of Physics **10**, 115008 (2008).
  - [6] Gert-Ludwig Ingold, P. Hanggi, and P. Talkner, Phys. Rev. E **79**, 061105 (2009).
  - [7] S. T. Smith and R. Onofrio, Eur. Phys. J. B **61**, 271 (2008).
  - [8] Q. Wei, S. T. Smith, and R. Onofrio, Phys. Rev. E **79**, 031128 (2009).
  - [9] J. Rosa and M. W. Beims, Phys. Rev. E **78**, 031126 (2008).
  - [10] H. Hasegawa, Phys. Rev. E **83**, 021104 (2011).
  - [11] A. Carcaterra, and A. Akay, Phys. Rev. E **84**, 011121 (2011).
  - [12] H. Hasegawa, J. Math. Phys. **52**, 123301 (2011).
  - [13] H. Hasegawa, Phys. Rev. E **84**, 011145 (2011).
  - [14] C. Jarzynski, Phys. Rev. Lett. **78**, 2690 (1997); Phys. Rev. E **56**, 5018 (1997).
  - [15] M. Thorwart, M. Grifoni, and P. Hänggi, Annals Phys. **293**, 14 (2001).
  - [16] H. Hasegawa, arXiv:1205.2058.
  - [17] L. Gammatoni, P. Hänggi, P. Jung, and F. Marchesoni, Rev. Mod. Phys. **70**, 223 (1998).
  - [18] P. Hänggi, F. Marchesoni, and P. Grigolini, Z. Phys. B **56**, 333 (1984).
  - [19] P. Hänggi, P. Jung, C. Zerbe, and F. Moss, 1993, J. Stat. Phys. **70**, 25 (1993).

- [20] L. Gammaitoni, E. Menichella-Saetta, S. Santucci, F. Marchesoni, and C. Presilla, Phys. Rev. A **40**, 2144 (1989).
- [21] A. Neiman and W. Sung, Phys. Lett. A **223**, 341 (1996).
- [22] H. Hasegawa, arXiv:1203.0770.
- [23] L. E. Reichl and W. M. Zheng, Phys. Rev. A **29**, 2186 (1984).
- [24] In the CL model ( $N_S = 1$  and  $N_B \rightarrow \infty$ ), we assume  $c_n = a/\sqrt{N_B}$  ( $a$ : constant) because the kernel  $\gamma(t)$  includes the  $c_n^2$  term as given by  $\gamma(t) = \sum_{n=1}^{N_B} c_n^2 (\cos \omega_n t / m \omega_n^2)$  which becomes  $\gamma(t) = (2/\pi) \int J(\omega) (\cos \omega t / \omega) d\omega \propto \delta(t)$  in the limit of  $N_B \rightarrow \infty$ ,  $J(\omega)$  denoting the spectral density [see Eq. (20)].
- [25] A careless mistake was realized in  $f_B(u)$  of Fig. 6(c) in Ref. [10], which should be nearly the same as that of Fig. 10(b) in this paper.
- [26] The recurrence time in a finite system is finite in the Poincaré recurrence theorem: H. Poincaré, Acta Math. **13**, 1 (1890), see also S. Chandrasekhar, Rev. Mod. Phys. **15**, 1 (1943).
- [27] A. K. Pattanayak and W. C. Schieve, Phys. Rev. Lett. **72**, 2855 (1994).